CSK SCIENTIFIC PRESS

Volume 3 | issue 1 Review Article

JOURNAL OF ENGINEERING, TECHNOLOGY AND APPLIED SCIENCES

On Start-Up Optimization for A 300mw Steam Turbine

Wei Wang[1], Chao Dong and Yongjian Sun[1]*

School of Electrical Engineering, University of Jinan, WestRoad of Nan Xinzhuang, Jinan, 100190, Shandong, China.

Corresponding Author: Yongjian Sun School of Electrical Engineering, University of Jinan, West Road of Nan Xinzhuang, Jinan, 100190, Shandong, China.

Submitted: 12 April 2025 **Accepted:** 27 April 2025 **Published:** 02 May 2025

Citation: Wei Wang, Chao Dong and Yongjian Sun (2025), On Start-Up Optimization for A 300mw Steam Turbine. Research Article. Journal of Engineering, Technology and Applied Science 3(1).01-21

Abastract

The start-up optimization of a steam turbine means that the maxi-mum stress value is within the limit value, and the start-up time is the shortest. The essence of this problem is a nonlinear problem with multiple local optimal solutions. This paper proposed a new mathemat- ical model to solve this problem. Based on the actual operating rules of a 300MW steam turbine, this paper has formulated 15 cold start-up schemes, and then established a 3-D model of the rotor using ANSYSto conduct thermal analysis and stress analysis. Taking the analysisresults of 15 start-up schemes as sample data, support vector machine was used to calculate future stress. Then use the adaptive weighted par-ticle swarm optimization algorithm to solve the initial parameters to obtain the new cold start-up time parameters. It verified that under the condition that the maximum stress value within the limit value, the start-up time is 32 minutes shorter than the initial scheme. Under this condition, the economic benefits of the power plant are improved

Keywords: 300MW Steam Turbine, Start-Up Optimization, Finite Element Analysis, Thermal Stress

Introduction

For steam turbine in thermal power plant, the ultimate goal of optimization is to reduce the stress value and start-up time of rotor. In the unit, the rotor of steam turbine is an important part, which carries the energy and torque [1]. The safety of steam turbine unit is mainly determined by the quality of turbine.

Article Title

rotor. Reducing the start-up time of the equipment is a decisive factor while ensuring that the stress value of the turbine rotor is less than the yield limit value of the rotor material. From a few years ago to now, the quality of life has improved significantly, the grid capacity has increased significantly, so the peak value of the grid has been increasing [2]. Frequent peak shaving operation means frequent start-up and shutdown of the steam turbine unit. The change of working condition of steam turbine unit will cause the damage of rotor material, thus shortening the life of the unit. The parameters of steam turbine will change greatly during start-up. Among them, the change of temperature parameter is the most important. It will make the rotor produce a force, which is called thermal stress. At the same time, it will make the metal material deform, mainly in the form of expansion deformation. Once the thermal stress exceeds the yield limit of the rotor material, the high-temperature components, mainly the turbine rotor, will produce certain damage, which will eventually bring some security risks [3].

The needs of today's society should be met, so it is necessary and very important to study the rapid start-up process. The start and stop of steam turbine depend on how long it can be used, which means that it directly affects the life of the unit. After a detailed study of the start and stop of the steam turbine unit, a curve of start-up is given and used to guide the unit, which can improve security and economy at the same time. In brief, the start- up optimization of steam turbine is to optimize a function. At the same time, this function has constraint conditions. Generally speaking, the start-up time is the shortest and the stress is within a reasonable range [4]. Before that, there were many ways to optimize start-up of unit. It is impractical to measure and test the input data in the actual power plant, so using complex simulation software is the most commonly used method to evaluate the solution.

The safe and trouble-free start-up of the unit, especially the steam turbine rotor, is often an important factor to limit the load change rate of the unit or increase the acceleration during the start-up process. Janusz et al. proposed that there is no conflict between the optimization of steam turbine start-up and the improvement of economy [5]. Henryk et al. through the measurement of arm temperature, the thermal stress of main components after heating is mon- itored, and the attention to the efficiency

and life of steam turbine unit is also given [6,7]. In this paper, the author focuses on the largest load components in the boiler, that is, the pipe fittings and the interface area. Through the research results, the author further demonstrates the best characteristics of the steam temperature and the main steam pressure, so as to promote the rapid start- up of the boiler. However, the experiment is only carried out in the selected designated area, and the experiment assumes that the heat load of the sys- tem is uniform, so the result error is relatively large. The drastic temperature change of turbine rotor in a short time will lead to the increase of temperature gradient, which will lead to higher thermal stress. Many researchers have stud- ied the optimization of heating rate. Taler et al, proposed a new optimization

Article Title

That the thermal stress is considered in the start-up optimization of boiler tur- bine system [8]. Green function and pontryagin maximum principle are used. However, in the analysis process of this paper, the author mainly focuses on a certain region of the rotor, and determines the rotor thermal stress accord- ing to the simplified thermal calculation analysis. This method speeds up the measurement speed, but this method has great limitations. Turbine rotor is a very complex structure, and this method is more suitable for simple geometry. Ji et al. proposed a method to optimize the starting process by monitor- ing several points with high rotor stress level [9]. In this paper, a start-up plan based on multiple temperature rise rates is proposed, and the relationship between steam temperature and maximum stress is determined by regression model. PSO algorithm is used to deal with the problem of cold start-up opti- mization to find the best temperature rise rate. In this paper, the temperature rise rate is taken as the parameter and the temperature rise rate is converted into time to calculate the total starting time, which increases the calculation amount. Therefore, this paper directly analyzes the temperature rise time of the stage when analyzing the problem, eliminating the conversion process of temperature rise rate and time. Du et al. a nonlinear model predictive control (MPC) rotor is proposed. The rotor is equivalent to a cylinder with external heat transfer and optimized shortening the start-up time [10] proposed and its effectiveness is proved.

In all the above research work, any work assumes that the initial temper- ature is horizontal, which assumption is a conventional assumption, because there is no temperature data when the turbine is shut down, and the process is very long. The most important turbine rotor is the main load-bearing part, and it cannot be installed with measuring devices. Because the initial state of cold start is different, the initial temperature field of turbine rotor is very different. The different initial thermal state will affect the initial stress field. The optimum temperature of the gas turbine inlet of the cycle is discussed in reference [11]. In the research of this paper, the state of the middle and high-pressure rotor during the cold start-up of the steam turbine is analyzed. Ana- lyze thermal stress every minute during the entire cold start-up process, so that the transient characteristics during the start-up can be captured. In fact, the analysis of steam turbine unit by finite element software is based on the model of steam turbine rotor. Furthermore, using the BP neural network to predict the analysis results, and a prediction model is generated. The stress value is predicted by the prediction model, and the accuracy of the model is tested. Finally, the optimal cold start-up curve is optimized by particle swarm optimization combined with the prediction model, and further verified by ANSYS.

Cold Start-Up Mathematical Model

The start-up time data of 300MW steam turbine are collected from con- ventional power plants, as shown in the figure 1. With the passage of time.

Article Title

the temperature and pressure of the boiler gradually increase. When the main steam temperature of the boiler reaches 260 ◦C, the steam pressure reaches 9.35Mpa, and the turbine (turbine rotor) starts to rotate. The steam pres- sure is not higher than 0.8MPa, and the vacuum of condenser is more than -0.04Mpa. When the rotor speed of the turbine is increased to 2054r / min, the temperature rise rate of the main steam temperature is 1.54 ◦C/min. When the main pressure reaches 370 ◦C, it starts to calculate the warm-up time of the medium speed. During the medium speed warm-up period, the time is 50mins. After the medium speed warm-up, the main temperature continues to heighten. When the speed of the turbine rotor reaches 2942r / min, the turbine unit starts to be connected to the grid. Under different heating time conditions, the main steam temperature rises to 538◦C within 550mins, and then the load of the unit in one hour reaches 74.67% of the total load, that is 224MW, when the start-up is completed. Besides the warm-up process, shorten the phase time of the start-up process can shorten the start-up time of the whole unit start-up process. As a result, the energy consumption is reduced and the economy of the power plant is improved. However, if the start-up time is shortened, it means that the temperature change rate as well as the steam pressure will increase, which will directly lead to the increase of rotor stress, and will undoubtedly have a greater impact on the service life of the rotor. According to the above discussion, considering the start-up process of the unit in the power plant, the thermal stress value of the rotor is calculated and ana- lyzed. Combined with the stress, the more optimized start-up parameters are designed to improve the start-up efficiency of the unit. The energy consump- tion of turbine start-up process is effectively reduced, and it is safer and more efficient, and the above conditions are met at the same time.

The essence of steam turbine start-up optimization is that the rotor mate- rial is within the stress range, minimize start-up time. Therefore, this problem can be transformed into the following equation eq.1 optimization problem.

$$\min J(t_1, t_2, \ldots, t_K) = \alpha_1 \frac{D_i}{D_{lim}} + \alpha_2 \frac{\sum_{i=1}^{K} t_i}{t_0} + \alpha_3 K \quad (1)$$

$$s.t. \begin{cases} D_i \le D_{lim} \\ T_{end} \le 538\,^{\circ}C \\ n_i \le 3000 \\ t_i > 0 \\ K \ge 3 \end{cases}$$

The sum of α1, α2 and α3 is equal to 1. A corresponds to the weight of damage and B to the weight of time. In this paper, α1 and α2 are all set as 0.45, α3 as 0.1 and K as 6, and the temperature is 538◦C.

Finite Element Calculation

The finite element analysis method increases the geometric details and refines the mesh division, which makes the analysis of higher-order potential

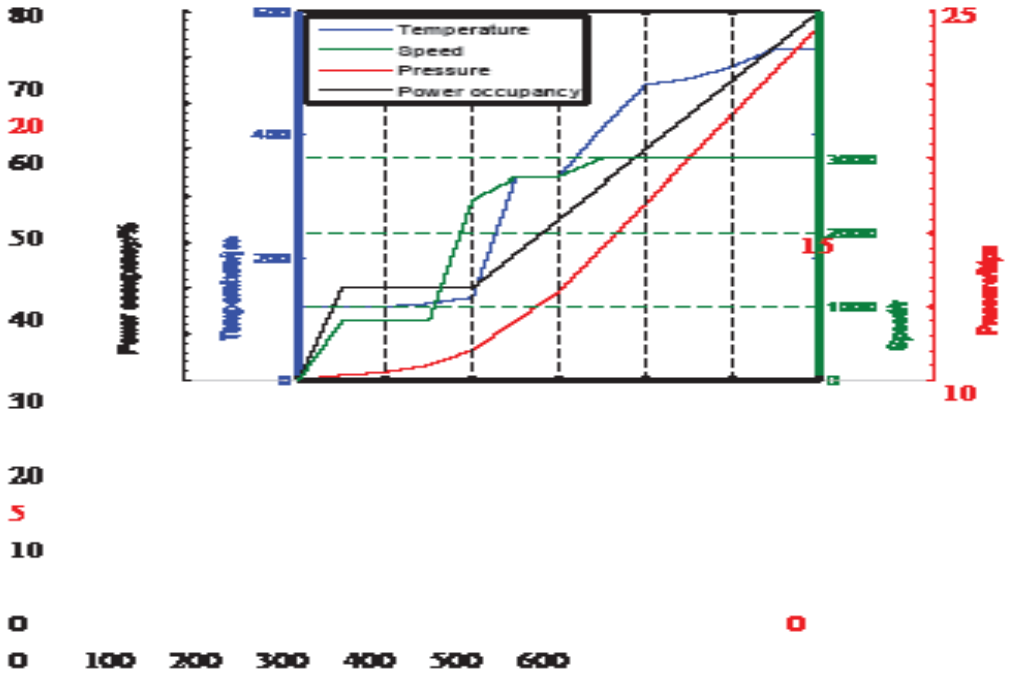

Figure 1: Cold Start-Up Curve of Standard Operating Condition

Elements more accurate [12]. Considering the above factors, this paper uses the commercial ANSYS to analyze and calculate the reasonably simplified turbine rotor.

Rotor Model and Finite Element Analysis

Based on the structural characteristics of the actual turbine rotor, estab- lish the rotor 3-D model by software. Because the 3-D modeling is closer to the actual operation results, so using the ANSYS to analyze the rotor 3-D model. In the process of 3-D modeling, the part of the rotor is reasonably sim- plified, which saves part of the calculation cost and the premise is to ensure the accuracy of the results. The ANSYS is used to analyze the three-dimensional model, and the temperature distribution and stress distribution of the three- dimensional model are calculated. There are 240456 nodes and 280875 meshes in the model. To ensure the accuracy of the results, the hexagonal structure is used in the mesh division. As shown in figure2, the material of the turbine rotor is 30Cr1Mo1V steel. Physical properties and chemical composition of materials are shown in table 1 and table2. When the finite element software is used for analysis, the physical properties of 30Cr1Mo1V steel change with temperature as shown in table3[13].

The rotor of steam turbine is reasonably assumed to be a non-heat source phenomenon, and then the rotor temperature is calculated. Based on the law of conservation of energy and fourier, the formula eq.2 for calculating the rotor

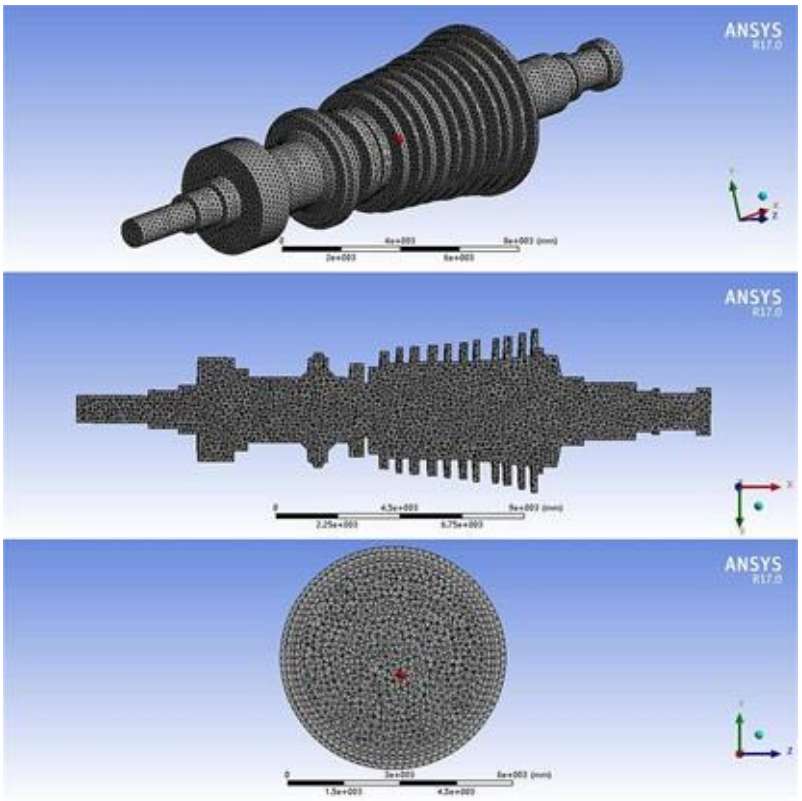

Figure 2: Turbine Rotor Model

Table 1: The 30cr1mo1v Steel Chemical Composition 1

Element	C	Fe	Mo	Cr	Si	Mn	P	S	V	Ni
Wt /% 0.28	1.10	0.28	0.73	1.13	0.023	0.22	0.005	0.24	0.4	

Table 2: The 30cr1mo1v Steel Chemical Composition 2

Temperature ◦	Yield strength σs	Ultimate strength σb	Elongation δ	Reduction of area ψ
20 C	629Mpa	779Mpa	20%	60%
◦				
540 C	465Mpa	520Mpa	29.6%	88.5%

Table 3: The Physical Property of 30cr1mo1v Steel

Temperature	20 C°	100 C°	200 C°	300 C°	400 C°	500 C°	600 C°
Young modulus E	214Gpa	212Gpa	205Gpa	199Gpa	190Gpa	178Gpa	178Gpa
Poisson ratio μ	0.288	0.292	0.287	0.299	0.294	0.305	0.305
Thermal conductivity λs	48.5W/m·K	47.1W/m·K	44.8W/m·K	42.8W/m·K	40.3W/m·K	37.5W/m·K	35.3W/m·K
Linear expansion coefficient αl	0	11.99	12.81	13.25	13.66	13.92	14.15
Specific heat c	554J/Kg	574J/Kg	599J/Kg	624J/Kg	666J/Kg	720J/Kg	804J/Kg

Article Title

Temperature Distribution is as Follows.

$$\begin{bmatrix} c_{11} & c_{12} & \cdots & c_{1n} \\ c_{21} & c_{22} & \cdots & c_{2n} \\ c_{31} & c_{32} & \cdots & c_{3n} \end{bmatrix} \begin{bmatrix} \dot{t}_1 \\ \dot{t}_2 \\ \dot{t}_3 \end{bmatrix} + \begin{bmatrix} K_{t11} & K_{t12} & \cdots & K_{t1n} \\ K_{t21} & K_{t22} & \cdots & K_{t2n} \\ K_{t31} & K_{t32} & \cdots & K_{t3n} \end{bmatrix} \begin{bmatrix} t_1 \\ t_2 \\ t_3 \end{bmatrix} = \begin{bmatrix} Q_1 \\ Q_2 \\ Q_n \end{bmatrix}$$

where, [c] is the matrix representing the specific heat capacity, [t] is the deriva- tive matrix of temperature, [K_t] is the matrix of heat conduction, [t] is the temperature value with direction, [Q] is the heat flux in the direction of the belt. n represents the dimension of the matrix, and the number of nodes inthe model is the value of n.

The initial boundary conditions of the rotor are set according to the equation eq.2, and the temperature distribution of the whole rotor is expressedby nodes, the time step of the integral part is different between two adja- cent times. According to the relationship between stress and strain, geometric equation and balance equation, the thermal stress distribution of rotor can be obtained.

$$\frac{\partial E}{\partial t} = \int_{r_i}^{r_o} 2\pi r \left[\frac{1}{r_o - r_i} \int_{r_i}^{r_o} t \, dr - t \right] dr \quad (4)$$

$$\frac{\partial E}{\partial t} = \frac{2\pi}{r_o^2 - r_i^2} \int_{r_i}^{r_o} t \, dr \quad (5)$$

Boundary Definition Conditions

The distribution of temperature of rotor is uneven. Centrifugal force and steam pressure affect the mechanical stress and thermal stress of rotor respectively [14]. The accurate boundary conditions directly affect the calcula- tion of temperature distribution and stress distribution. The axis of the rotor shall be parallel to the y-axis. Based on the structure and heat conduction char- acteristics of steam turbine rotor, the boundary conditions can be established as follows.

Thermal Boundary

(1) The surface temperature of turbine rotor is set as initial temperature. Under cold start-up, the temperature of the shaft body is about room temper- ature, so the loading ambient temperature is 25 ◦C, the loading temperature of the outer surface is 50 ◦C before the regulating stage, the sealing temperature is 120 ◦C, and the outlet temperature of high and medium pressure is 100 ◦C.

(2) The contact surface between the two ends of the rotor and the air is small, so the two ends of the rotor can be set as the insulation surface.

(3) The external surface boundary condition of rotor is the transfer relation of the third kind of boundary condition of known steam temperature.

Article Title

(4) The rotor has no central hole, so there is no heat source at the axis, so the temperature parameter is only applied from the outer surface.

The above boundary conditions and initial temperature are loaded into the 3-D model to establish the cold start-up model

Structure Boundary

The structural boundary conditions of the rotor model are shown in table3. It is difficult to calculate the start-up data by using the conventional calcu- lation formula, especially when the steam turbine unit is under 80% load. The problem of small flow rate can be calculated by pressure data and temperature coefficient. During start-up and stopping the steam turbine unit, the steam temperature, steam pressure and steam flow on the surface of rotor change.

The heat transfer coefficient of rotor can be calculated by ANSYS, which is mainly based on the temperature distribution and material properties.

Coefficient of Thermal Conductivity

Nt•l
β —— (W/m •
R• ³ • C) (6)

When Re ≤2.4*105, Nt=0.675R0.5. When Re >2.4*105, Ny=0.217R0.8.
where, Re = ub Ra , Rb , outer radius of the turbine rotor blade, l , thermal conductivity of the steam, c , kinematic viscosity of the steam, ub , the circum- ferential velocity of the rotor blade radius, and the unit of the circumferential velocity is m/s.

Thermal Conductivity of The Shaft

Nt•λ
α —— (W/m •° C) (7)
R• ²

Article Title

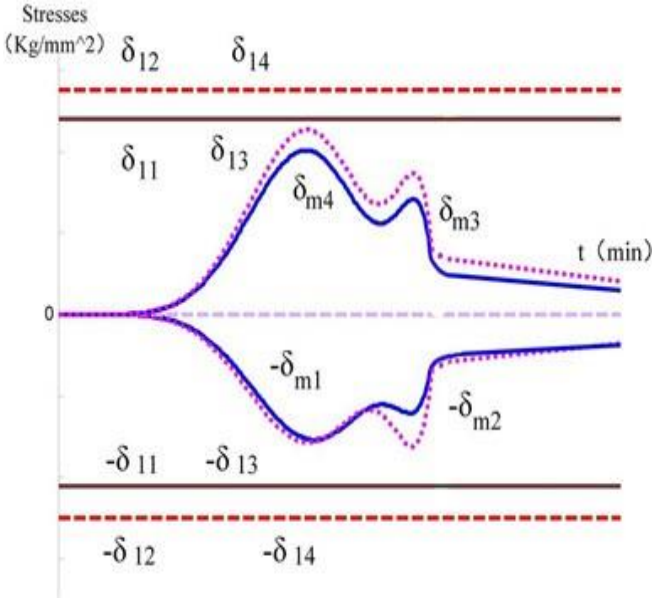

Figure 3: Variation Trend of Maximum Thermal Stress of Rotor

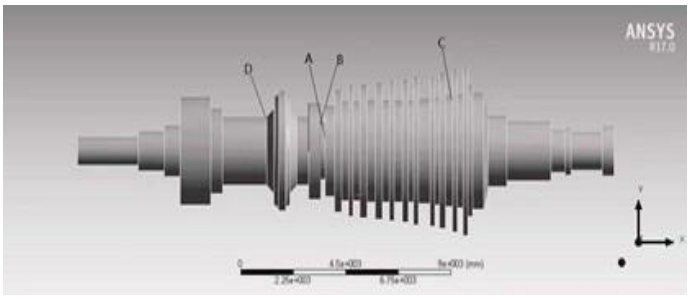

Figure 4: Location of Thermal Stress Monitoring Points

Points does not exceed the maximum stress that the material can bear, the stress at other parts is also safe. The analysis results of the whole cold start-up process are shown in figure5, and the stress value under the original condition is shown in figure6.

From the results, four points A, B, C, D are processed in turn, and the thermal stress changes of the regulating stage, the front groove of the regulating stage and the root of the blade can be seen. It can be seen from the above pictures that during the rotor whole start-up process, the max stress value appears at point A, and the maximum value is 446.24Mpa. Compared with the start-up curve in figure1. After warm-up at medium speed, the maximum.

Article Title

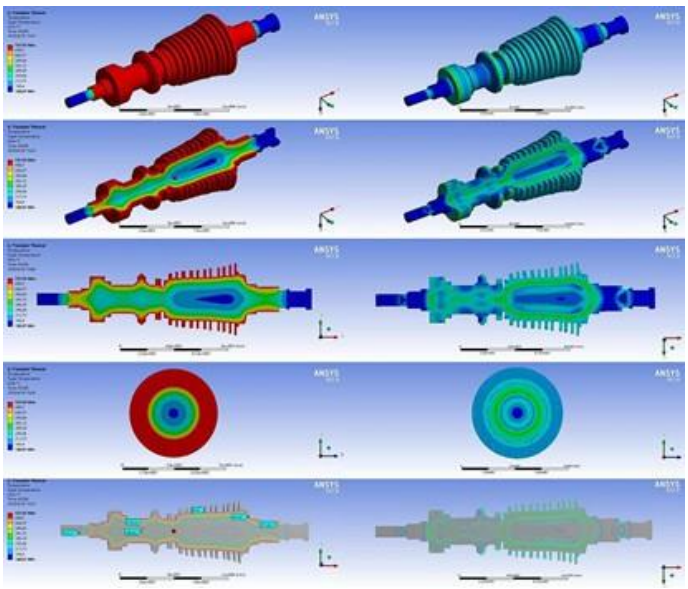

Figure 5: Turbine Rotor Model for Finite Element Analysis

Stress Curve of Original Working Condition

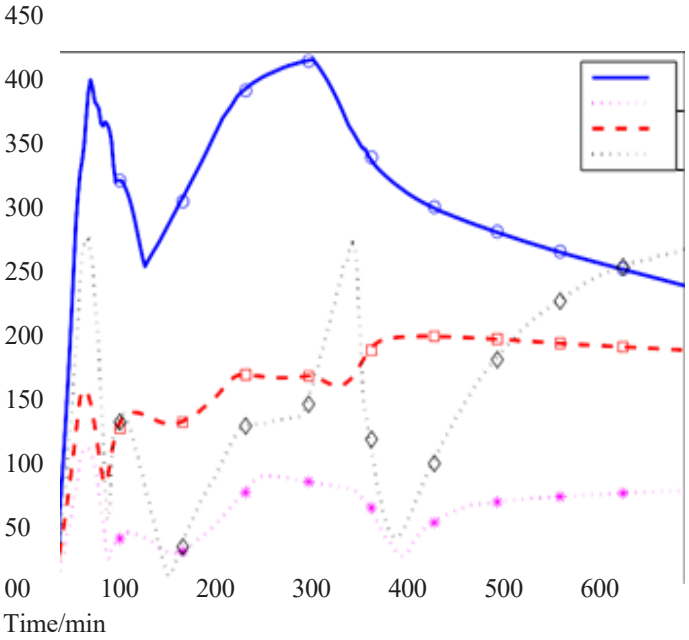

Figure 6: Thermal Stress Curve Under Original Working Condition

thermal stress of rotor appears. With the increase of speed, the derivative of temperature on the outer surface increases. The thermal stress value of start- up process is analyzed, the maximum thermal stress is far from reaching the limit stress value, which leads to a long time of start-up process, the start-up curve in the initial conditions is too smooth, and the start-up efficiency of the whole unit is poor.

Cold Start-Up Optimization of Turbine Rotor

Cold Start-Up Sample Data

In the unit start-up process, the unit start-up time is too long, and the original start-up scheme is more conservative. During the start-up process, the rotor is greatly affected by temperature, and the derivative of temperature is proportional to the thermal stress [17]. Therefore, reducing the start-up time reasonably and increasing the life loss of the turbine rotor properly can reduce the energy consumption during start-up, and at the same time supply power to the outside more quickly, so that the benefit index of power plant has been improved [18].

Based on the start curve under the initial condition, as shown in figure1, the temperature rise time of each state is shortened, and 15 start conditions are determined. According to the 15 cold start schemes, the maximum stress value of each scheme is obtained by the ANSYS.

The relevant parameters of the start-up scheme about 15 working condi- tions and the maximum stress value under each condition are shown in table4. The stress values of different cold start schemes are shown in figure7. Because the stress changes obviously from the middle speed warm-up, our working condition only aims at the temperature rising section after the middle speed warm-up, i.e., t1, t2, t3, t4, t5, t6. Taking different start-up schemes of t1 to t6 as the sample data, the stress prediction models of the rotor are established by using BP neural network and SVM respectively, and the prediction models are compared and analyzed.

Schedule	t1 /min	t2/min	t3 /min	t4/min	t5/min	t6 /min	σm/Mpa	start-up time/min
1	49.9	50.6	47.6	49.1	48.6	49.0	447.35	584.2
2	48.7	51.0	46.5	47.2	49.4	50.0	449.96	581.3
3	48.5	50.7	47.4	48.5	49.1	49.7	447.38	582.2
4	48.7	50.9	46.4	49.9	49.2	48.5	448.89	579.3
5	48.8	50.2	47.3	49.4	48.7	49.0	448.78	577.6
6	47.8	50.1	49.2	48.7	47.6	48.9	451.02	574.2
7	48.0	46.8	48.8	47.3	46.5	48.4	449.21	581.1
8	45.3	48.2	49.9	46.3	45.4	48.2	453.59	576.4
9	46.7	48.9	48.3	47.4	48.8	49.3	452.87	579.9
10	47.3	48.9	45.8	46.7	47.5	46.9	457.35	575.2
11	46.8	49.7	47.7	48.8	47.3	49.6	450.66	578.7
12	43.2	44.6	47.2	44.3	47.8	44.7	459.82	571.1
13	46.3	50.0	42.7	49.5	46.7	48.9	453.35	578.3
14	45.8	49.9	46.4	47.8	46.4	48.9	454.18	574.4
15	47.4	46.5	48.3	44.6	49.3	48.8	449.69	576.4

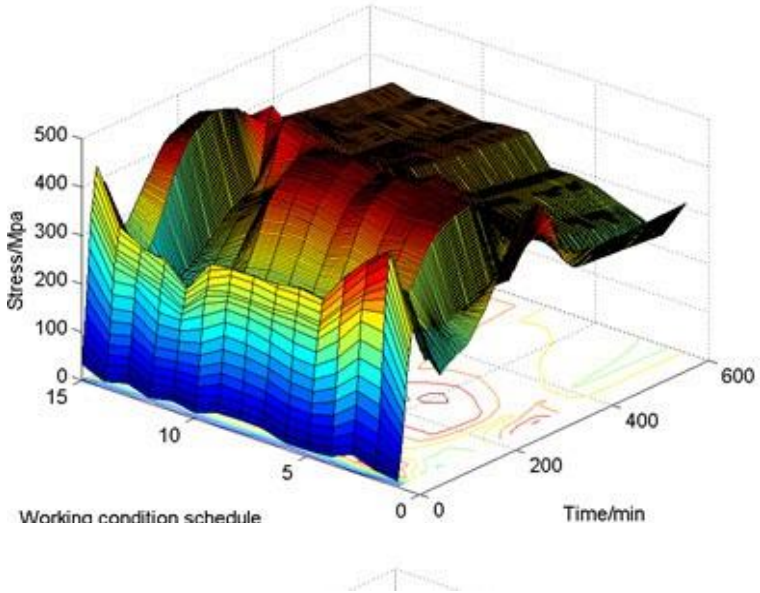

Figure 7: Maximum Thermal Stress of Rotor Under Different Cold Start-Up Schemes

BP neural network is a very convenient tool, it does not need complex mapping relations, knowledge through the training of data to form its own unique rules, forming a specific model, so that the input data to the model,the output results are closest to the expected results.

In this paper, the structure model of BP neural network uses three-layerstructure, which are input layer, hidden layer and output layer. From the firstlayer to the second layer, we need to set a weight. In this paper, we set theweight of this stage as f_{kn}, the hidden layer should set the threshold value ofthe nth neuron, which is set as γ_n. At the same time, a threshold should be set between the second layer and the third layer as m_{nj}, the threshold of thejth neuron in the output layer is set as σ_j. In the structure diagram of BPneural network, there are a total of d input neurons, representing d dimension.There are q hidden neurons in total. Each hidden neuron has its corresponding threshold. There are j output neurons, so there are j output neuron thresholds.

where, X is the input of neural network. The input data of this paper is six periods of time, that is, dimension d is 6 and Y is output. Every six groups oftime parameters correspond to a maximum thermal stress value, that is, the output dimension j is 1, the calculation process of neural network is shown in the following e.8.

1. From input layer to hidden layer

$$\varepsilon_a = \sum_{k=1}^{n} f_{ka} * X_i \quad (8)$$

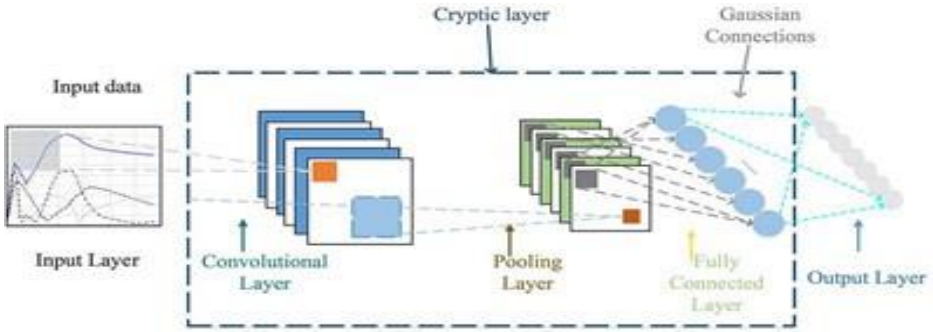

Figure 8: BP Neural Network Structure

$$|X_1\ X_2\ X_3\ \ldots\ X_d| = \begin{vmatrix} f_{11} & f_{12} & f_{13} & \ldots \\ f_{1q} & f_{21} & f_{22} & \\ f_{23} & \ldots & f_{2q} & f_{31} \\ f_{32} & f_{33} & \ldots & f_{3q} \\ \cdot & \cdot & \cdot & \cdot \\ \cdot & \cdot & \cdot & \cdot \\ \cdot & \cdot & \cdot & \cdot \\ f_{d1} & f_{d2} & f_{d3} & \\ \ldots & f_{dq} & & \end{vmatrix} \quad (9)$$

2. Calculation of path hidden layer

$$b_q = f(\varepsilon_a - \gamma_a) \quad (10)$$

3. Hidden layer to output layer

$$\xi_j = \sum_{n=1}^{q} m_{qj} * b_q \quad (11)$$

$$|b_1\ b_2\ b_3\ \ldots\ b_q| = \begin{vmatrix} m_{11} & m_{12} & m_{13} & \ldots \\ m_{1j} & m_{21} & m_{22} & m_{23} \\ \ldots & m_{2j} & m_{31} & m_{32} \\ m_{33} & \ldots & m_{3j} & \\ \cdot & \cdot & \cdot & \cdot \\ \cdot & \cdot & \cdot & \cdot \\ \cdot & \cdot & \cdot & \cdot \\ m_{q1} & m_{q2} & m_{q3} & \ldots \\ m_{qj} & & & \end{vmatrix} \quad (12)$$

4. Calculation of output hidden layer

$$Y_{jk} = f(\xi_j - \sigma_j) \quad (13)$$

where, εn is input of the nth hidden neuron, fkn is weight function from the first layer to the second layer, bq is activation function of hidden layer, ξj is weight function from the second level to the third degree, σj is activation function of output neurons.

The above is the calculation process of neural network training. At this time, it is necessary to add termination conditions, that is, to set the error size and iteration number. In this paper, the error is set to 0.03, the maximum iteration number is set to 1000 generations, the training results are displayed once every 100 steps, and the learning rate is set to 0.1. When the maximum number of iterations is satisfied or the error range is satisfied, the program output is terminated. The neural network adopts a three-layer structure, with six inputs in each group, namely six time periods, and one output. Six time periods are a start-up process, and six time periods correspond to a maximum stress. There are 15 groups in total, of which 10 groups are used for training and 5 groups are used for testing.

In order to establish a high precision and high stability prediction model, it is a good choice to use the BP neural network prediction function and SVM prediction function. Combining the corresponding optimization algorithm with BP neural network can further improve the accuracy.

Next, we do a comparative experiment between neural network and support vector machine.

Comparison Experiment1: Bp Neural Network and Support Vector Machine of Laplace Kernel Function

BP neural network is used to make a prediction model, and the results of the prediction model are obtained to analyze the feasibility of the results of the neural network. In the training process, the maximum number of iterations is set to 1000 generations, and the training results are displayed once every 100 steps. The learning rate is set to 0.1, and the error is set to 0.03. 10 groups of maximum stress values of 15 groups of sample data are taken as the training data, and 5 groups are taken as the test data. The results after the neural network training are shown in figure9 and figure10.

SVM is used as a prediction model. In this paper, the laplace kernel function form is shown in eq.14. The former 10 working conditions are the training data and 5 groups are the test data. The parameters are set as follows, the initial weight W of the prediction model is set to 15.4, the cross-validation multiple is 6, and the prediction model with penalty parameter C of 3.9642 is established. The training set coefficient of determination of the model is 0.99994, the test set mean square error of is 0.0078006, and the coefficient of determination is 0.93086. The curves of the model's pre-test set and training set are shown in figure 10 and figure11.

$$k(a, b) = \exp(-a-b) \qquad (14)$$

where, a is a point existing in the empty concept, b is the center point of the kernel function, which is also in the space, and δ is the width parameter, the performance of the function decreases with the increase of δ. In the above picture, mse is the mean square error, R^2 is the determination coefficient, and the calculation formula of mean square error and determination coefficient is.

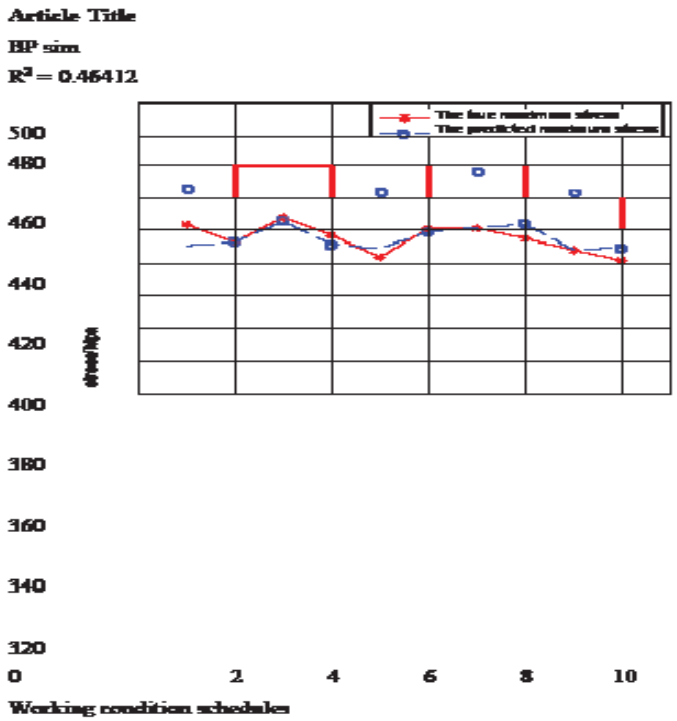

Figure 9: BP Train Result

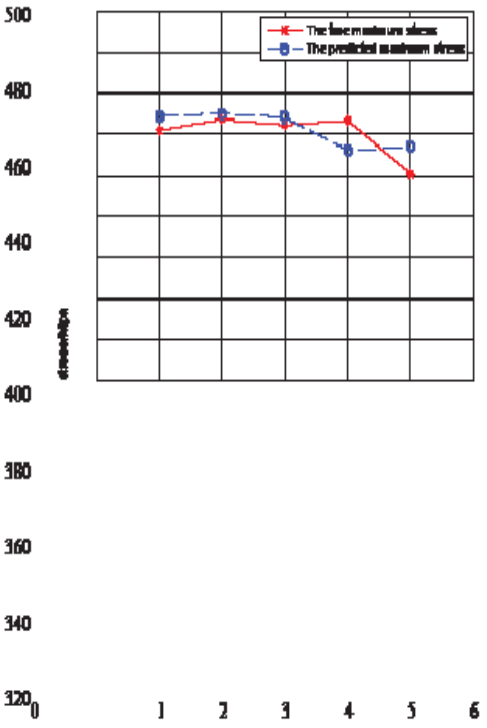

Fig. 10: BP test result

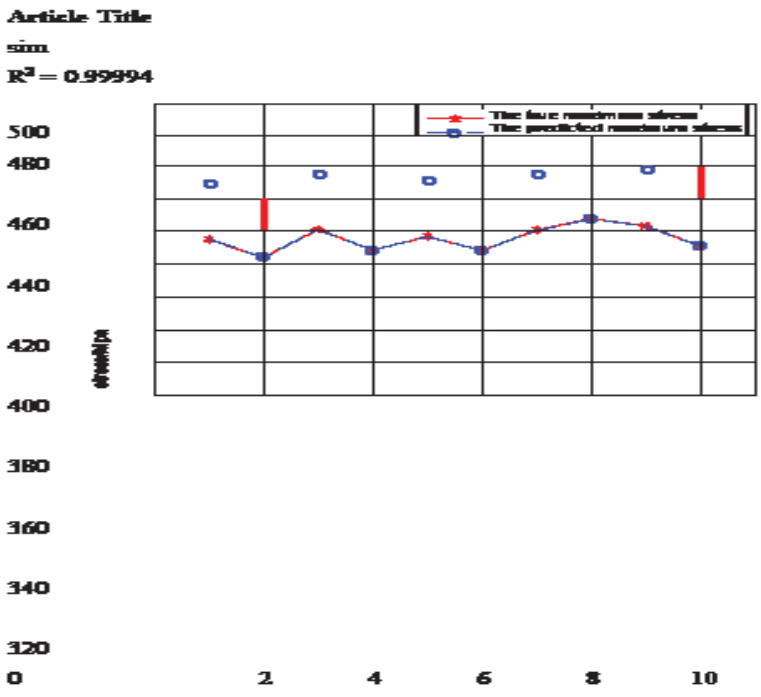

Figure 11: SVM Training Result

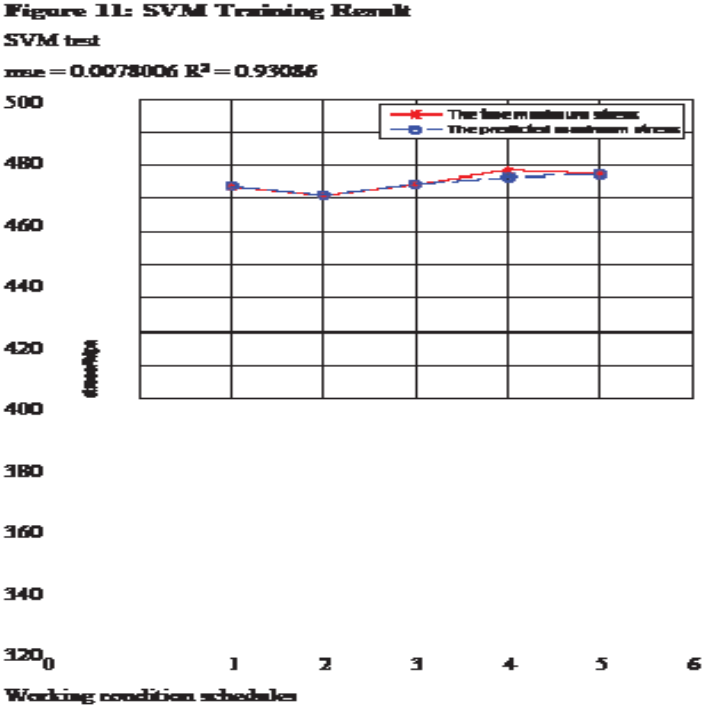

Figure 12: SVM Test Result

as follows eq.15 and eq.16.

$$mse = \frac{1}{n}\sum_{i=1}^{n}(s_i - s_i)^2 \quad (15)$$

$$R^2 = \frac{\sum_{i=1}^{n}(s_i - \bar{s}_i)^2}{\sum_{i=1}^{n}(s_i - \bar{s}_i)^2} \quad (16)$$

where, n is the number of test data, s_i is the actual data, s_i is the predicted data, $\bar{s}_i$ is the mean value of the data.

Comparison Experiment2: With Support VectorMachine of RBF

Before this paper, some researchers used RBF radial basis function, also known as gaussian kernel function. The gaussian kernel function is shown in eq.17.

$$k(a, b) = \exp \left(-\frac{\|a-b\|}{\delta^2} \right) \quad \text{---(17)}$$

where, a is a point existing in the empty concept, b is the center point of the kernel function, which is also in the space, and δ is the width parameter, the performance of the function decreases with the increase of δ.

In this paper, the results of support vector machine with gaussian kernel function and support vector machine with laplacian kernel function are com- pared. The prediction results of support vector machine with Gaussian kernel function are shown in figure13 and figure14.

In the support vector machine of gaussian kernel function, the mean square error of training results is 0.0348572, and the coefficient of determination is 0.942565. The mean square error of test results is 0.032482 and the coefficient of determination is 0.815037. Obviously, this problem is more suitable for laplace kernel function to solve.

After the comparison of the two prediction models, it is obvious that the prediction model made by SVM of laplace kernel function algorithm is better. Because the sample data is too small, the neural network prediction results are not satisfactory. The actual thermal stress values of the five-working con- ditions are respectively 446.2Mpa, 448.9Mpa, 448.8Mpa, 454.3Mpa, and the predicted stress values are respectively 446.16Mpa, 448.84Mpa, 448.81Mpa, 454.37Mpa. The prediction errors of the five groups were 0.0089%, 0.0013%, 0.04%, and 0.85% respectively. The errors are all within a reasonable range, and the accuracy of the model is verified by the errors.

Start Planning Based on Particle Swarm Optimization

Particle swarm optimization, is a kind of random search algorithm based on the cooperation of group examples, which is developed by the behavior of birds foraging. It is also a kind of swarm intelligence. Particle swarm opti- mization is an evolutionary algorithm. The essence of evolutionary algorithm

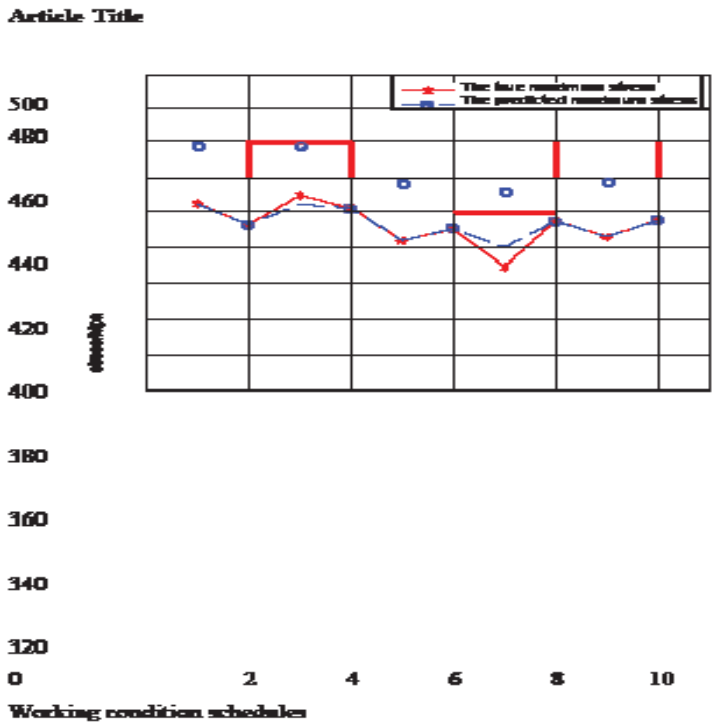

Figure 13: Training Results of Gaussian Kernel Function

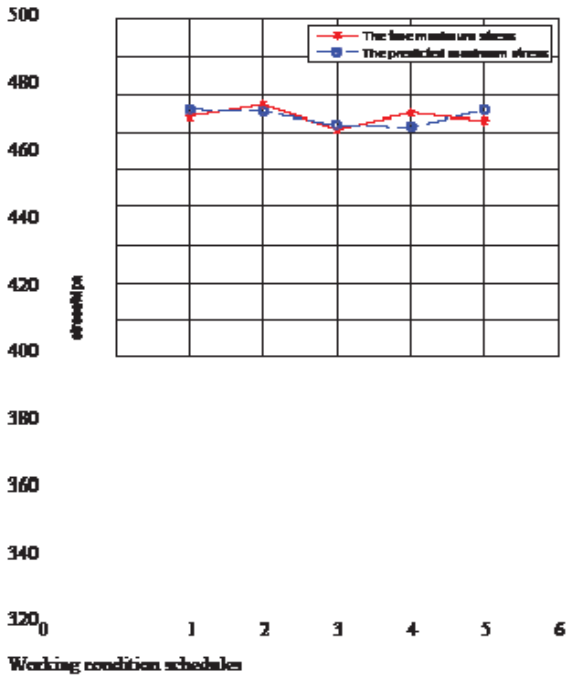

Figure 14: Test Results of Gaussian Kernel Function

is an adaptive. It is an evolutionary algorithm that compares the solution of an optimization problem with that of an individual, and applies it to the reor- ganization, selection and variation of the solution in the optimization process. By simulating the reproduction, compilation and competition of organisms to reflect the optimization problem, the continuous updating of variables is real- ized and the optimal solution is finally obtained. Particle swarm optimization algorithm has many advantages mainly manifested as high efficiency, good at optimizing nonlinear problems, as it can be simple implementation.

In this paper, the adaptive inertia weight of particle swarm optimization algorithm is used, the ordinary particle swarm optimization algorithm is fixed weight, but in the actual optimization process, the number of iterations con- tinues to increase, the details of the solution will also change, so if the weight value is fixed, there will be many deficiencies in the overall solution process, resulting in poor optimization effect, change to dynamic weight After that, the optimization process will dynamically adapt to some details of the solution process, making the optimization effect better.

Adaptive weight PSO algorithm PSO algorithm. Particles have the ability to expand the search space and have a faster convergence speed. The formula is shown in eq.18.

$$vi = K[vi+\phi 1 random(0, 1)(pbesti-xi)+\phi 2 random(0, 1)(gbesti-xi)] \quad (18)$$

$$K = \sqrt{2 - \phi - \phi 2 - 4\phi}\ \phi = \phi 1 + \phi 2, \phi > 4$$

where, K is the convergence factor to ensure convergence, ϕ is the parameter associated with K to determine the value of K, for the convergence factor K to good work, it is necessary to make K greater than 0.5. Therefore, the association parameter a must be greater than 4. In this paper, ϕ is 4.1, then K is 0.729. v_i represents the flying speed of particle i, x_i represents the position of the ith particle, $pbest_i$ represents the optimal position on the path of the ith particle, $gbest_i$ represents the optimal location of all paths, random(0, 1) represents a random number, between 0 and 1. The optimization algorithm mainly has the following two steps,

- Calculate and determine the parameters, number and speed of each particle.
- Set the number of iterations until the stop condition is reached or understood within the set value.

The optimization part of this paper adopts adaptive weight particle swarm optimization algorithm. The implementation process of PSO is as follows, the maximum number of iterations was set as 200, and the size of the population was set as 60. In the 53 generation, the optimal solution appears, and the corresponding fitness function value is 8.024, as shown in figure15. Optimiza- tion is done under constraints. And finally, we get the optimal solution. The optimized time of PSO is shown in table5.

Article Title

Table 5: Start-Up Parameters and Thermal Stress of Adaptive Particle Swarm Optimization

t1/min	t2/min	t3 /min	t4 /min	t5 /min	t6/min	stress/Mpa
44.2	43.2	45.4	47.2	45.3	47.8	464.72

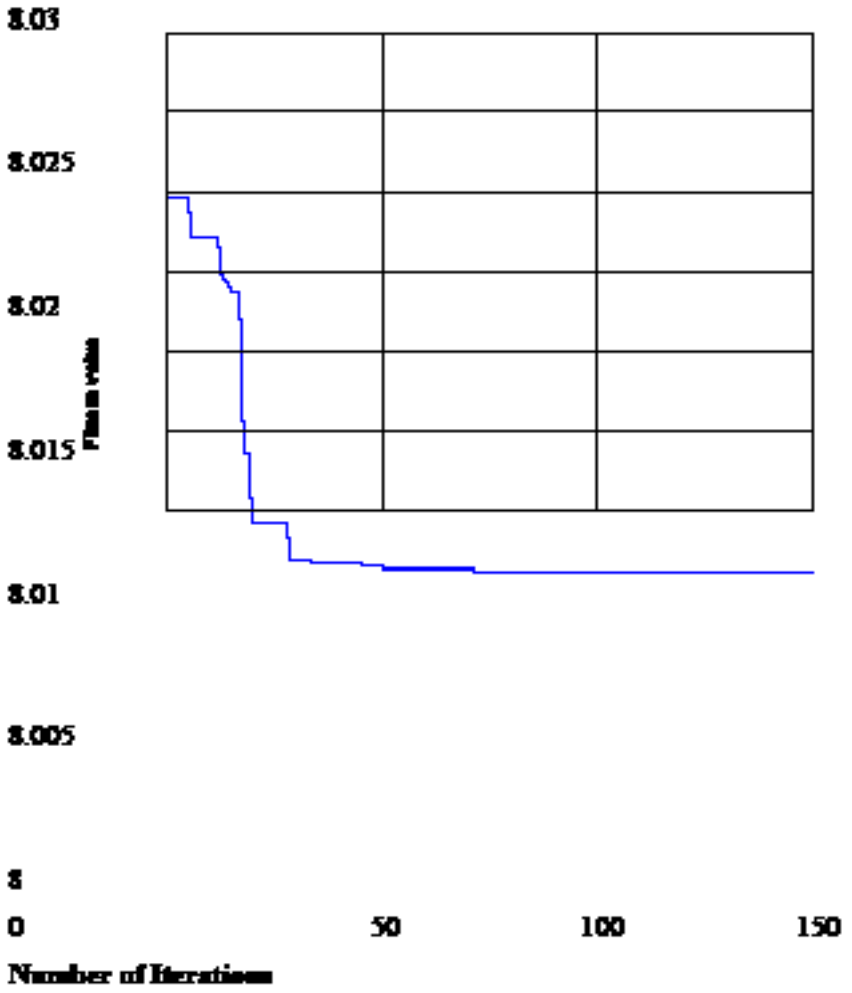

Figure 15: Fitness Evolution Curveof Adaptive Weight Particle Swarm Optimization

Comparison Experiment3: With Conventional ParticleSwarm Optimization Algorithm

The weight value of conventional particle swarm optimization algorithm is fixed and will not change with the change of fitness value. It directly sets afixed value, namely ω. The formula of conventional particle swarm optimizationalgorithm is as follows eq.19.

$$v_i = \omega v_i + c_1 r_1 (pbest_i - x_i) + c_2 r_2 (gbest_i - x_i) \qquad (19)$$

The results of the conventional particle swarm optimization algorithm are shown in figure16. Compared with the particle swarm optimization algo- rithm with adaptive weights, the iteration times are more and the calculation is slower. The optimization results of the conventional particle swarm opti- mization algorithm are not as good as those of the adaptive particle swarm optimization algorithm. The detailed optimization results of the conventional particle swarm optimization algorithm are shown in table6.

Table 6: Start-Up Parameters and Thermal Stress of Conventional ParticleSwarm Optimization

t1/min	t2/min	t3 /min	t4 /min	t5 /min	t6/min	stress/Mpa
44.6	41.6	46.4	45.6	45.4	48	454.2

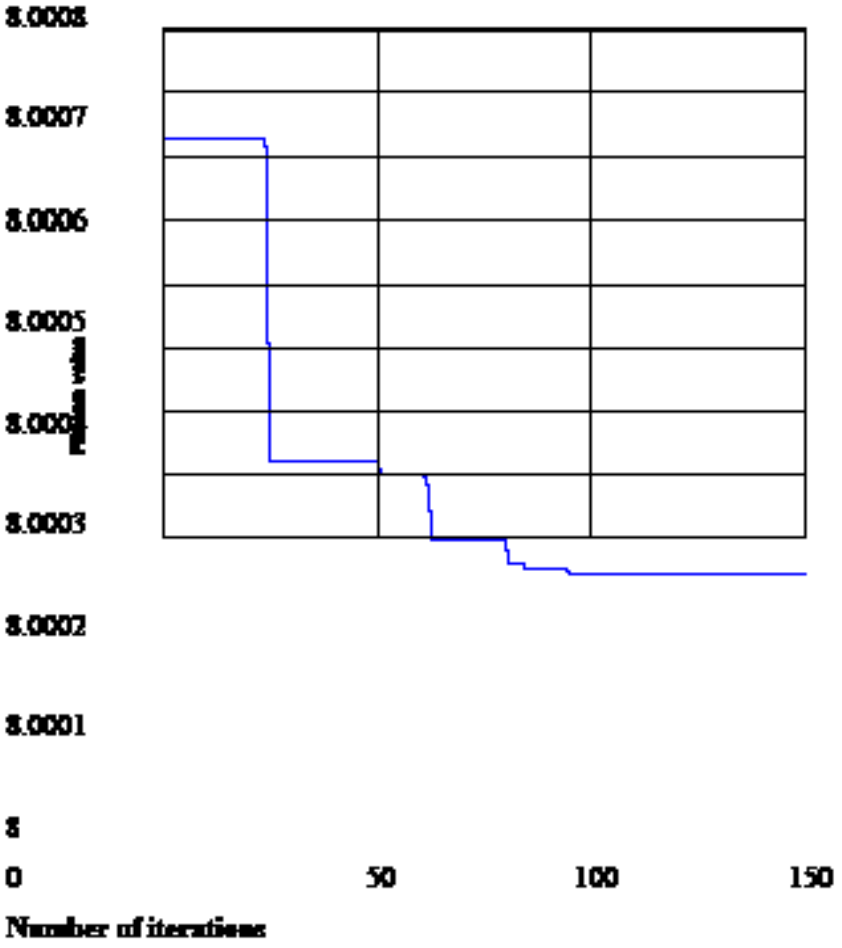

Figure 16: Conventional Particle Swarm Optimization Fitness Evolution Curve

In the conventional particle swarm optimization algorithm, the learning factors c1 and c2 are set to 1.4925, the maximum number of iterations is set to 150, and the weight ω is set to 4.1. Finally, the optimization results are obtained in the 94th generation, and the fitness value is 8.0006. From the comparison results, it is not difficult to see that the optimization results of the particle swarm optimization algorithm with adaptive weights are more suitable for the optimization of the model, with fewer iterations and more reasonable results.

Stress Verification of Optimized Start-Up Time

In this paper, particle swarm optimization (PSO) is used to obtain a set of start-up time parameters. Under the optimal cold start-up parameters, the start-up time of the unit under the original conditions was shortened by 32mins and 5.3%, as shown in figure17. ANSYS was used to calculate the rotor stress during the new start. The positions of the 4 monitoring points remain unchanged, and the stress results are blowing figure18. As can be seen from figure18, the maximum stress value of the rotor under the new start-up scheme is 464.72Mpa, which appears in the temperature rise period after the.

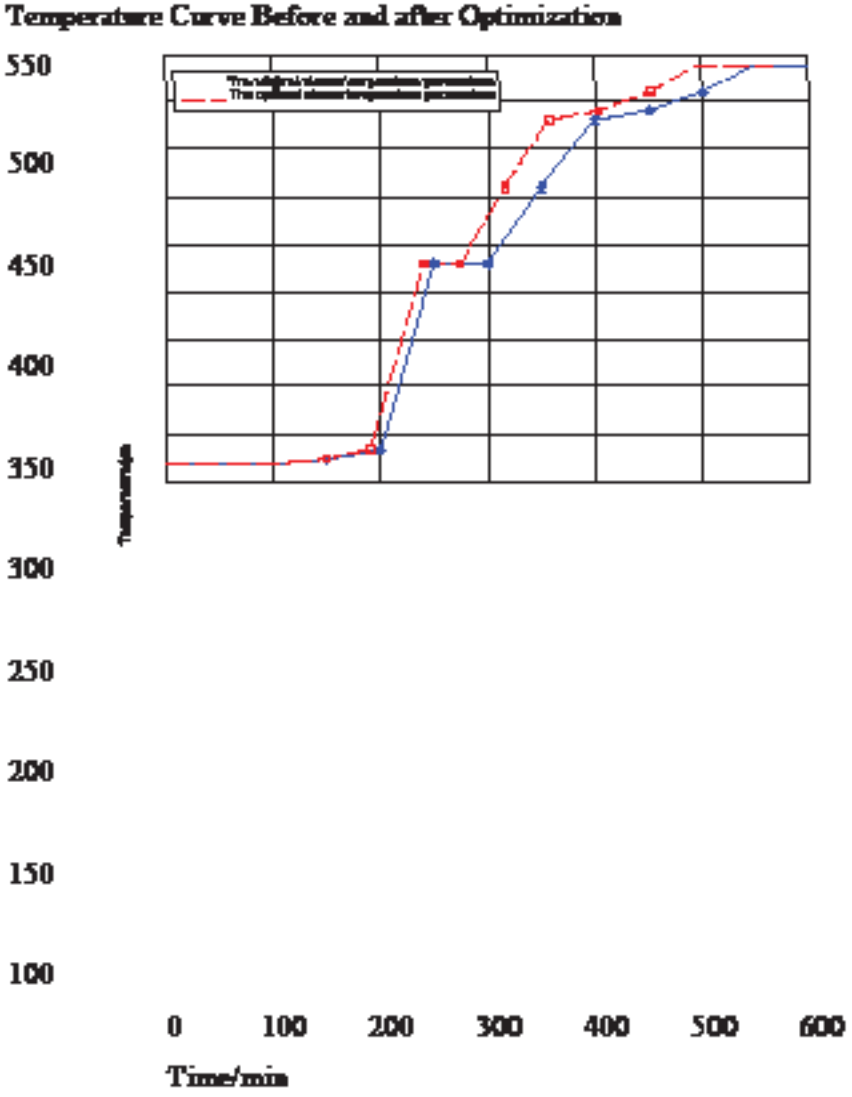

Figure 17: Comparison Between the Optimized Scheme and the Original Scheme

Medium-speed turbine preheats. The calculation results of the stress field are shown in figure18.

The partial stress field of the rotor is shown in figure19. Through the picture of the stress field, the position of stress concentration can be clearly seen.

As shown in above figure, the stress concentration part can be seen clearly. According to the above data, the time parameters after adaptive particle swarm optimization meet the accuracy requirements. According to the opti- mized start-up plan, the whole start-up process of the unit is shortened by 32 minutes, and the load of the unit is greatly increased. The optimization results are satisfactory. The start-up time and energy consumption of the unit are reduced, also the safety of the unit is guaranteed, the economy is improved, and the benefit of the power plant is further improved.

Conclusion

The reasonable optimization and new start-up scheme can ensure that the unit of the power plant starts quickly under the safe and economic conditions. Therefore, it is necessary to study the cold start-up scheme of 300MW rotor. And obtain the final optimal startup scheme. The research work of this paper is as follows.

1.t1, t2, t3, t4, t5, t6 being used represents the start-up time of the stage and proposes an optimal function, t1, t2, t3, t4, t5, t6 represents the tem- perature rise time of six rising stages respectively, and the objective function represents the shortest start-up time. The optimization results are carried out under the actual constraints.

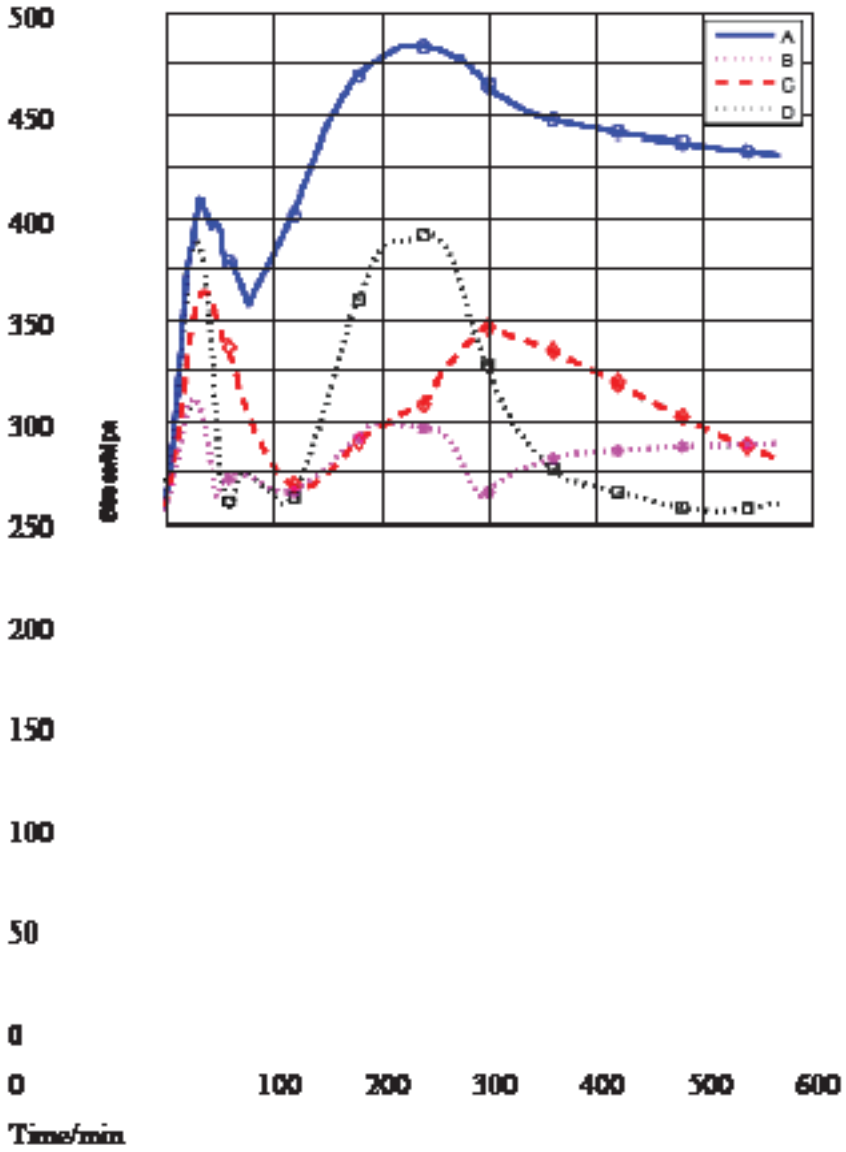

Figure 18: Stress Value of Monitoring Point Under Cold Start-Up OptimalScheduling

2. 15 kinds of cold start-up conditions are established, and the stress field of rotor is analyzed by ANSYS.

3. Based on the finite element analysis results of 15 start-up schemes, BP neural network and two kinds of support vector machines are used to establish the prediction model of starting time and maximum thermal stress on rotor surface. The two support vector machine models are gaussian kernel function and laplacian kernel function. At the same time, the three prediction models are compared with each other. Finally, it is proved that the SVM based on laplace kernel function is better, and the prediction error is less than 0.3%.

4. On the basis of considering the results of the prediction model, the par- ticle swarm optimization algorithm is used to obtain the initial parameters. The particle swarm optimization uses the adaptive weight particle swarm opti- mization algorithm, and makes the results of the conventional particle swarm optimization algorithm. The two results are used to compare, highlighting the advantages of the adaptive particle swarm optimization algorithm.

The time parameters after particle swarm optimization meet the accuracy requirements. According to the optimized start-up plan, the whole start-up process of the unit is shortened by 32 minutes, and the load of the unit is greatly increased. The ANSYS is used to verify the optimized start-up scheme. In which it finds that the stress value of the max stress concentration point of the turbine rotor meets the requirements well.

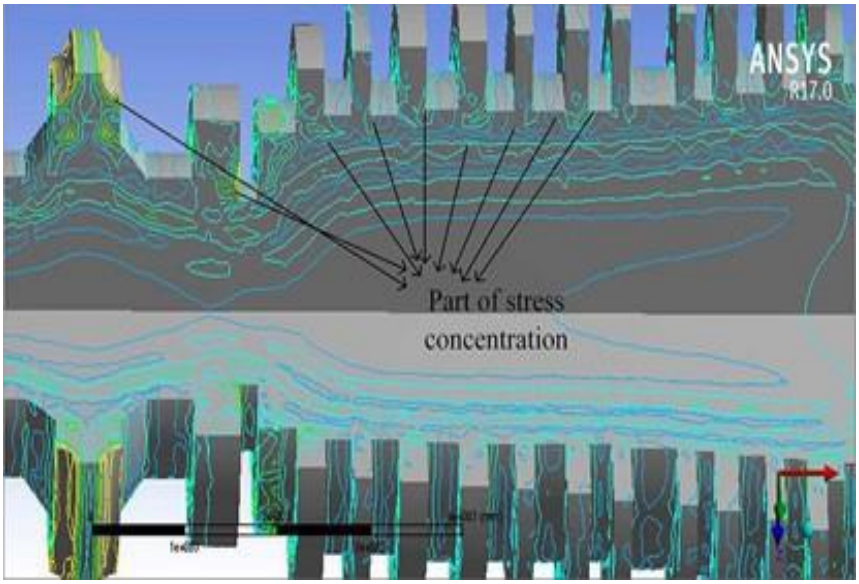

Figure 19: Local Stress Distribution of Rotor

Author Declarations

Ethical Approval: not applicable. This article does not involve human subjects or animals.

Competing Interests: the author has no relevant financial or non-financial interests that need to be disclosed, and no competitive interests related to thisarticle.

Authors' Contributions: Wang Wei is responsible for building the framework and writing of the article. Li Shaohui is responsible for collecting and sorting documents. Sun Yongjian is responsible for providing ideas and formulating research directions.

Funding: this work is supported by National Natural Science Foundation (NNSF) of China under Grant 61603149, by Shandong Key Research and Invention Program under Grant 2019GSF111046, by the Science Foundation for Post Doctorate Research from the University of Jinan.

Availability of Data and Materials: data sharing is not applicable to this article as no new data were created or analyzed in this study.

References

1. Ahmed Azeez a, Robert Eriksson a, Daniel Leidermark a, Mattias Calmunger b (2020) Low cycle fatigue life modelling using finite element strain range partitioning for a steam turbine rotor steel, Theoretical and Applied Fracture Mechanics 113: 311-323.
2. Jakub Pawlicki, Dominik Głowacki, Janisław Zwoliński, Artur Mościcki (2020) Elastic limit load resource when reaming holes in turbine rotor discs, Engineering Failure Analysis 113: 104555.
3. Zhewen Chen a, Yanjuan Wang, Xiaosong Zhang (2020) Energy and exergy analyses of SCCO2 coal-fired power plant with reheating processes, Energy 211: 118651.
4. Hong H, Wang W, Liu Y (2019) High-temperature fatigue behavior of a steam turbine rotor under flexible operating conditions with variable load- ing amplitudes, International Journal of Mechanical Sciences 163: 105121.

5. Janusz K, Mateusz B, Marcin J (2018) The thermodynamic and economic characteristics of the modern combined cycle power plant with gas turbine steam cooling, Energy 164: 359-376.
6. Henryk Z, Andrzej R (2018) The impact of the control method of cyclic operation on the power unit efficiency and life, Energy 15: 565-574.
7. Jan Taler, Dawid Taler, Karol Kaczmarski, Piotr Dzierwa, Marcin Trojan, et al. (2018) Monitoring of thermal stresses in pres- sure components based on the wall temperature measurement, Energy 160: 500-519.
8. Jan Taler, Piotr Dzierwa, Dawid Taler, Piotr Harchut (2015) Optimization of the boiler start-up taking into account thermal stresses, Energy 92: 160-170.
9. Ji Dong-mei, Sun Jia-qi, Sun Quan, Guo Heng-Chao, Ren Jian-xing., et al. (2018) Optimization of start-up scheduling and life assessment for a steam turbine, Energy 160: 19-32.
10. S. Dettori, A Maddaloni, V Colla, O Toscanelli, F Bucciarelli, et al. (2019) Nonlinear Model Predictive Control strategy for steam turbine rotor stress, Energy 158: 5653- 5658.
11. Seik Park, Jugon Shin, Mitsuhiro Morishita, Toshihiko Saitoh, Gyungmin Choi, et al. (2019) Validation of measured data on F/A ratio and turbine inlet temperature with optimal estimation to enhance the reliability on a full-scale gas turbine combustion test for IGCC, International Journal of Hydrogen Energy 44: 13999-14011.
12. Lei Zhao, Lianyong Xu, Yongdian Han, Hongyang Jing, Zhifang Gao (2019) Modelling creep-fatigue behaviours using a modified combined kinematic and isotropic harden- ing model considering the damage accumulation, International Journal of Mechanical Sciences 161: 105016.
13. Mariusz B (2018) The low-cycle fatigue life assessment method for online mon- itoring of steam turbine rotors. International Journal of Fatigue 113: 311-323.
14. Saboya B I, Egido I, Lobato M E (2019) MOPSO-tuning of a threshold- based algorithm to start up and shut-down rapid-start units in AGC, International Journal of Electrical Power and Energy Systems 108: 153-161.
15. S Cano, JA Rodríguez, JM Rodríguez, JC García, FZ Sierra, et al. (2019) Detection of damage in steam turbine blades caused by low cycle and strain cycling fatigu, Engineering Failure Analysis 97: 579-588.
16. Yi Zhang, Benjamin Decardi-Nelson, Jianbang Liu, Jiong Shen, Jinfeng Liu (2020) Zone economic model predictive control of a coal-fired boiler-turbine generating system, Chemical Engineering Research and Design 153: 246-256.
17. Weijun L, Hui L, Tao C (2020) Process fault diagnosis with model- and knowledge-based approaches: Advances and opportunities, Control Engi- neering Practice 105: 104637.
18. Milad M, Ali C, Amin R (2018) An intelligent hybrid technique for fault detection and condition monitoring of a thermal power plant, Applied Mathematical Modelling 60: 34-47.